Catalytic Mechanism of *Escherichia coli* Glycinamide Ribonucleotide Transformylase Probed by Site-Directed Mutagenesis and pH-Dependent Studies†

Jae Hoon Shim and Stephen J. Benkovic*

Department of Chemistry, 152 Davey Laboratory, The Pennsylvania State University, University Park, Pennsylvania 16802

Received February 26, 1999; Revised Manuscript Received May 28, 1999

ABSTRACT: Site-directed mutagenesis followed by studies of the pH dependence of the kinetic parameters of the mutants has been used to probe the role of the active site residues and loops in catalysis by glycinamide ribonucleotide transformylase (EC 2.1.2.2). The analysis of the mutants of the strictly conserved active site residues, His108 and Asp144, revealed that His108 acts in a salt bridge with Asp144 as a general acid catalyst with a pK_a value of 9.7. Asp144 also plays a key role in the preparation of the active site geometry for catalysis. The rate-limiting step in the pH range of 6−10 appears to be the catalytic steps involving tetrahedral intermediates, supported by the observation of a pL (L being H or D)-independent solvent deuterium isotope effect of 2. The ionization of the amino group of glycinamide ribonucleotide both as a free and as a bound form dominates the kinetic behavior at low pH. The analysis of a mutation, H121Q, within the loop spanning amino acids 111−131 suggests the closure of the loop is involved in the binding of the substrate. The kinetic behavior parallels pH effects revealed by a series of X-ray crystallographic structures of the apoenzyme and inhibitor-bound enzyme [Su, Y., Yamashita, M. M., Greasley, S. E., Mullen, C. A., Shim, J. H., Jennings, P. A., Benkovic, S. J., and Wilson, I. A. (1998) *J. Mol. Biol. 281*, 485−499], permitting a more exact formulation of the probable catalytic mechanism.

Glycinamide ribonucleotide transformylase (GAR transformylase,[1] EC 2.1.2.2) catalyzes the first of the two formyl transfers in the de novo purine biosynthetic pathway and forms the C-8 atom of the purine ring. The formyl group is transferred from *N*10-formyl tetrahydrofolate to the amino group of glycinamide ribonucleotide (GAR) to form formylglycinamide ribonucleotide (fGAR) (Figure 1). GAR transformylase has been a target for developing novel antifolate drugs to be used in cancer chemotherapy. Because of its biological and pharmacological importance, the enzyme has been the subject of intensive studies on its structure and mode of action. These investigations have focused on the *Escherichia coli* enzyme which is a small monomer (23 kDa) (*1*, *2*) rather than a covalent constituent of the large trifunctional protein found in eukaryotes, yet exhibits a high degree of sequence homology and mechanistic similarity with respect to its eukaryotic counterpart (*3*, *4*).

X-ray structures of inhibitor bound in a binary or ternary complex have revealed three amino acid residues in the active site, His108, Asn106, and Asp144, that are strictly conserved (*5*, *6*). Site-directed mutagenesis studies have demonstrated the importance of these residues in catalysis (*7*). The formylation reaction is believed to proceed via a direct transfer mechanism probably involving a tetrahedral intermediate (Figure 1) (*8*, *9*). A preliminary pH−rate profile exhibited a pH maximum between pH 8.0 and 8.5 with a decrease in activity at the pH extremes (*10*). A study of the solution structure of GAR transformylase proposed that a pH-dependent dimer−monomer transition near physiological pH might act as a means of regulating the enzyme activity (*11*). Recently, however, a mutant enzyme, E70A, that maintains its monomeric structure over a wide pH range was found to have a pH−rate profile similar to that of the wild type, indicating that the pH-dependent dimer−monomer equilibrium is not coupled to enzymic activity (*12*). Instead, the analysis of the X-ray structure of E70A has revealed a marked difference in the tertiary structure between pH 3.5 and 7.5, leading to a proposal that a pH-dependent confor-

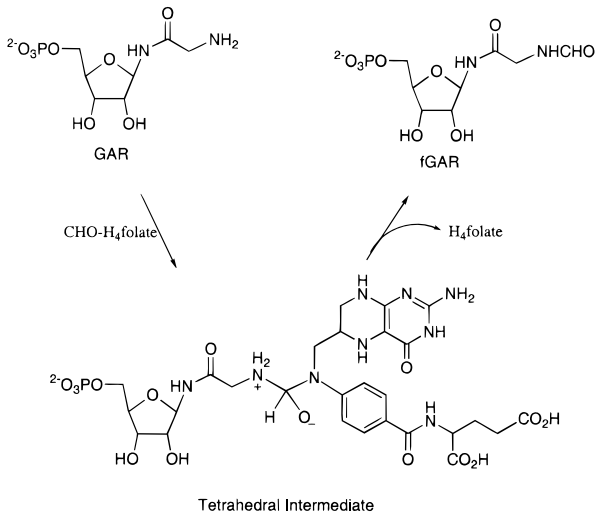

FIGURE 1: Reaction catalyzed by GAR transformylase with a tetrahedral transition state.

† This work was supported by PHS Grant GM24129 from the National Institutes of Health (S.J.B.).

* To whom correspondence should be addressed. Phone: (814) 865-2882. Fax: (814) 865-2973.

[1] Abbreviations: GAR, β-glycinamide ribonucleotide; fGAR, formyl-β-glycinamide ribonucleotide; GAR transformylase, glycinamide ribonucleotide transformylase; fDDF, 10-formyl-5,8-dideazafolate; IPTG, isopropyl β-D-thiogalactoside; LB, Luria broth; PCR, polymerase chain reaction; BW1476U89, Burroughs-Wellcome multisubstrate inhibitor.

10.1021/bi9904609 CCC: $18.00
Published on Web 07/13/1999

mational change might be responsible for the observed pH dependence of enzyme activity (*12*). Despite these efforts, little kinetic evidence exists that would explain the chemical role of the active site residues in the transformylation reaction. In this paper, we have investigated the pH-dependent kinetic behavior of the wild type and mutant enzymes, which, together with structural information, clarifies their function in the activity of GAR transformylase.

MATERIALS AND METHODS

Materials. Synthetic oligonucleotides were prepared by an Expidite 8909 DNA Synthesizer (Perceptive Biosystems, Framingham, MA). PCR primers were passed through a Sephadex G-25 column before being used. Restriction enzymes were obtained from Promega and New England Biolabs. T4 DNA ligase was purchased from Boehringer Mannheim. Taq polymerase and nucleotides were purchased from Promega. Agarose for gel electrophoresis was from Kodak; low-melting temperature agarose was from Bioproducts, and Ultrafree-MC filter units were from Millipore. QIA-tip plasmid purification columns were from QIAGEN, and a Wizard PCR Preps DNA Purification System was from Promega. Deuterium oxide (99.9 at. %) was purchased from Aldrich. GAR was prepared as described previously (*13*). The cofactor 10-formyl-5,8-dideazafolate (fDDF) was purchased from J. Hynes (Medical University of South Carolina, Charleston, SC). All other chemicals that were used were obtained from Fisher, VWR, Sigma, or Aldrich.

Bacterial Strains and Plasmids. The *E. coli* strains used for expression were TX680 and MW12 [TX680(DE3)] which are auxotropic cells for *pur*N and *pur*T genes (*7*). DH5α was used for preparation of plasmids. In general, the plasmid pJS167 (*2*) was used as a mutagenesis vector and the plasmid pMSW2 (*7*) was used as an expression vector in MW12 cells. For the expression of the H108A mutant, however, pJS167 was used in TX680 cells.

Site-Directed Mutagenesis. Site-directed mutagenesis was performed using the PCR overlap extension method as described previously by using the plasmid pJS167 as a template (*7*). PCR products were purified by using a low-melting temperature agarose gel and Wizard PCR Preps DNA Purification System. Digestion, ligation, and transformation were performed as described previously (*7*). Plasmid DNA was purified from transformants using QIA-tip 100 columns and sequenced. The correct mutant genes were cloned into a pMSW2 vector for expression.

Protein Preparations. Except for H108A, the GAR transformylase proteins were prepared by using a pMSW2 vector and IPTG induction of the T7 promoter in MW12 cells. These cells were grown in LB medium with 100 μg/mL ampicillin and 25 μg/mL kanamycin at 37 °C up to an OD_{600} of 0.5. Protein production was induced by adding IPTG (1 mM final concentration), and cells were grown for an additional 3.5 h at 37 °C. For the H108A mutant enzyme, the pJS167 vector was expressed using temperature induction of the λ_{PL} promoter in TX680 cells. These cells were grown in LB medium with 100 μg/mL ampicillin and 25 μg/mL kanamycin at 32 °C up to an OD_{600} of 0.5. Protein production was induced at 42 °C for 10 h.

Protein purification conditions were as previously described except that a Q-Sepharose column (2.5 cm × 15 cm) was used instead of a MonoQ column (*7*).

Kinetic Measurements. All kinetic measurements were performed at 25 °C in a buffer that contained 50 mM 2-(*N*-morpholino)ethanesulfonic acid, 25 mM ethanolamine, 25 mM Tris, and 100 mM sodium chloride (MTEN). The ionic strength of this buffer remains constant over the pH range that was used. Instead of the unstable natural cofactor, stable 10-formyl-5,8-dideazafolate (fDDF) which behaves kinetically as the natural cofactor was used in all kinetic measurements (*2*). Enzyme assays were carried out in a 1 mL cuvette thermostated on a Gilford 252 spectrophotometer by monitoring the production of DDF at 295 nm ($\Delta\epsilon = 18.9\ mM^{-1}\ cm^{-1}$). The value of $\Delta\epsilon$ remained unchanged over the pH range that was used. Initial velocity data were obtained at different pH values by varying one substrate with the other substrate at saturating concentrations. To ensure that the fixed substrate was saturating at each pH, individual reactions were repeated with higher concentrations of the fixed substrate, and no change in the rates was observed. The pH of the assay mixture was determined before and after the reaction. For deuterium oxide buffers, pD was measured by adding 0.4 to the pH meter reading.

Stopped-flow experiments were performed on an Applied Photophysics Kinetic Spectrometer (Cambridge, England) that has a thermostated sample cell. Absorbance measurements were conducted at 295 nm with a 1 mm slit width. Enzyme (14 μM final concentration) was preincubated with a saturating amount of GAR at each pH and reacted with a limiting amount of fDDF (2.4 μM final concentration). In most experiments, five to eight traces were recorded and averaged for data analysis. Data were collected over a given time interval by an Archimedes computer. All data were analyzed by a nonlinear least-squares computer program provided by Applied Photophysics.

Data Processing. Data were fitted to the appropriate equations using a nonlinear least-squares fitting program in KaleidaGraph (version 3.0). Data from saturation kinetics were fitted to the Michaelis−Menten equation to determine k_{cat} and K_m values. The data from the k_{cat}−pH profile for the wild type enzyme were fitted to eq 1, and those for the H108A and D144A mutants were fitted to eq 2. For the k_{cat}/K_m(fDDF) and k_{cat}/K_m(GAR) profiles, eq 3 was used to fit the data. The fDDF titration curve was fitted to eq 4. In eqs 1−4, y is the value of the kinetic parameter, C is the pH-independent value of y, H is the hydrogen ion concentration, and K_{a1} and K_{a2} are the acid dissociation constants.

$$\log y = \log[C/(1 + H/K_{a1} + K_{a2}/H)] \quad (1)$$

$$\log y = \log[C/(1 + H/K_{a1})] \quad (2)$$

$$\log y = \log\{C/[(1 + H/K_{a1})(1 + K_{a2}/H)]\} \quad (3)$$

$$\log y = \log[C/(1 + K_{a2}/H)] \quad (4)$$

RESULTS

Preparation of Mutant Enzymes. The mutant D144A and H121Q plasmids were constructed by the procedure of Warren et al. (*7*). Sequencing of the entire structural gene for all mutants confirmed that no other mutation, other than the desired one, is present. The mutant enzymes, H108A, D144A, and H121Q, were expressed in auxotropic *E. coli* cells which are free of wild type GAR transformylase

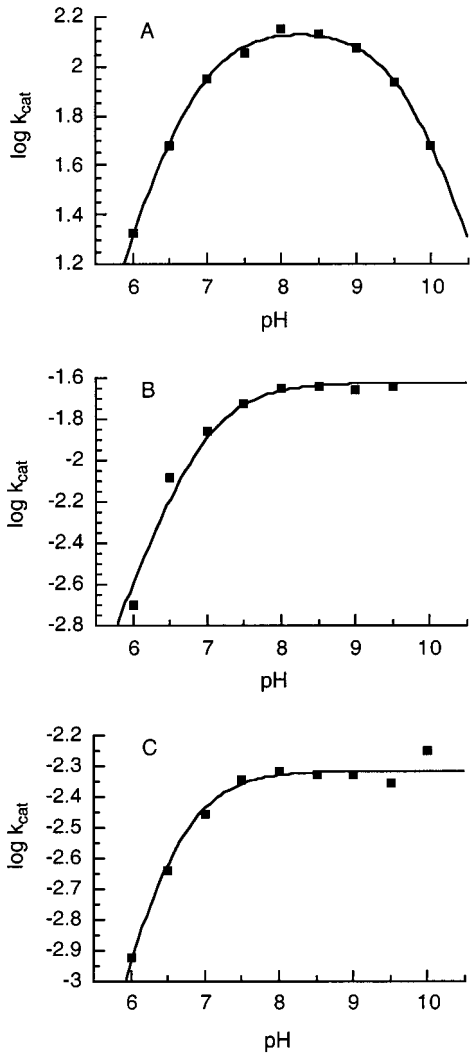

FIGURE 2: pH dependence of k_{cat} for the wild type (A), the H108A mutant (B), and D144A mutant (C). The solid line in panel A is fitted to eq 1, and those in panels B and C are fitted to eq 2.

expressed from the genomic DNA. These mutant and wild type enzymes were purified to homogeneity as described in Materials and Methods.

pH Dependence of k_{cat}. The pH dependence of k_{cat} for GAR transformylase is shown in Figure 2A. The data show a bell-shaped curve with limiting slopes of 1 on either side of the pH maximum. A nonlinear least-squares fit of the data to eq 1 yields two pK_a values, 6.8 ± 0.1 and 9.7 ± 0.1. The pH value for maximum activity is around 8.

The first question was whether the decline in velocity at either side of the pH maximum is due to an irreversible inactivation of the enzyme. To answer this issue, the enzyme was preincubated at various pH values in the range of 6−10 for about 15 min and the activity was rapidly measured after dilution into pH 8.0 buffer. All the samples that were tested regained full activity at pH 8.0, indicating that the decline in activity must result from improper ionic forms in the enzyme or substrates, not from the irreversible inactivation of the enzyme. Mutant enzymes used in this research were tested in the same manner and were found to be stable at pH 6−10.

The second question was whether one or both of the pK_a values corresponded to a change in the rate-determining step.

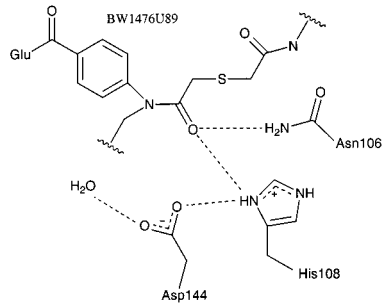

FIGURE 3: Diagram of the hydrogen-bonding interactions between the multisubstrate adduct BW1476U89 and the active site residues of GAR transformylase (*6*).

Table 1: Summary of Kinetic Parameters for GAR Transformylase at the pH Maximum (8.0)

	k_{cat} (s^{-1})	K_m(GAR) (μM)	K_m(fDDF) (μM)
wild type	133 ± 3	95 ± 6	21.1 ± 2.3
H108A	0.021 ± 0.002	115 ± 2	21.5 ± 2.5
D144A	0.0048 ± 0.0001	122 ± 3	28.4 ± 1.6
H121Q	80 ± 7	414 ± 29	99 ± 12

The study of the kinetic mechanism of GAR transformylase at pH 7.5 revealed that the k_{cat} value is predominantly determined by the rate of interconversion of the ternary complexes with random binding of substrate and cofactor (*13*). To determine whether this finding extended to other pH values, we carried out single-turnover reactions in the pH range of 6−10 to measure directly the rate of interconversion of the ternary complexes. The resulting k_{obs} values exhibited a pH−rate profile that is nearly identical to the k_{cat}−pH profile, demonstrating that k_{cat} values represent the catalytic step over this pH range. These observations established that the two pK_a values in the k_{cat}−pH profile must arise from the ionization of the groups within the ternary complex.

The crystal structures of binary or ternary complexes with the enzyme and a multisubstrate adduct inhibitor or a folate analogue and GAR have revealed that the active site contains two ionizable amino acid residues, His108 and Asp144, in such positions that they may assist the reaction (*5*, *6*). Figure 3 shows the hydrogen-bonding interactions of these residues with the multisubstrate adduct inhibitor BW1476U89 (*6*). The δ1 nitrogen of His108 forms two hydrogen bonds, one to the carbonyl oxygen of the inhibitor which is equivalent to the formyl oxygen in the folate cofactor and the other to the carboxylate of Asp144. It is very likely that His108 or Asp144 may participate in the catalytic mechanism and may be responsible for the observed pK_a values in the k_{cat}−pH profile. To test this possibility, we determined the pH−rate profiles for the mutant enzymes.

The k_{cat}−pH profile for the H108A mutant enzyme is shown in Figure 2B and is no longer a bell-shaped curve. Curve fitting with eq 2 gave a pK_a value of 7.0 ± 0.1 which overlaps with the acid side pK_a value in the k_{cat}−pH profile for the wild type. As expected from the previous study (*7*), this mutation caused a significant drop in k_{cat} by 4 orders of magnitude (Table 1). Interestingly, the D144A mutant exhibited a k_{cat}−pH profile very similar to that of H108A, with a pK_a of 6.5 ± 0.1 (Figure 2C). The activity of this mutant is also reduced significantly by 5 orders of magnitude. This result establishes that both active site residues, His108

Scheme 1: Mechanisms Involving Substrate Ionization[a]

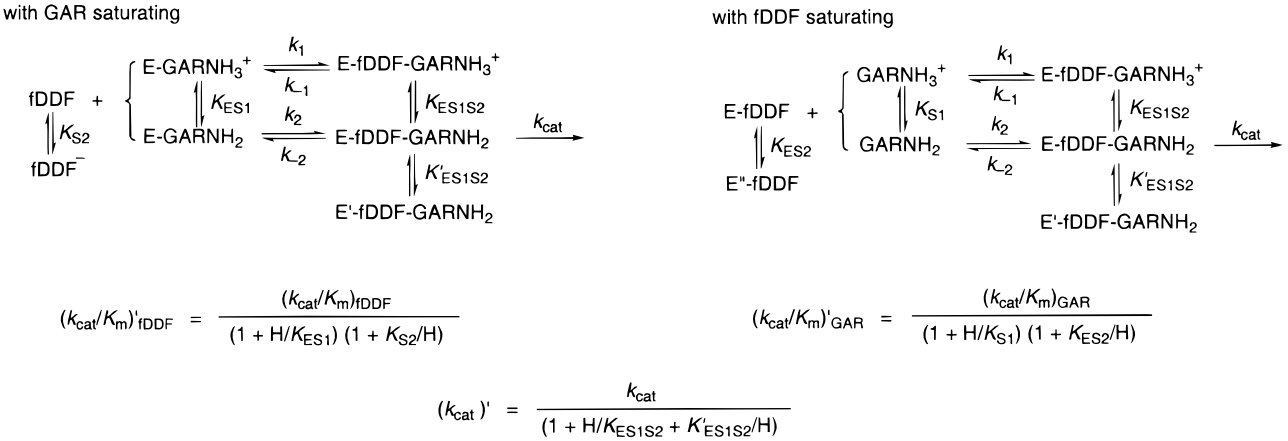

$$(k_{cat}/K_m)'_{fDDF} = \frac{(k_{cat}/K_m)_{fDDF}}{(1 + H/K_{ES1})(1 + K_{S2}/H)} \qquad (k_{cat}/K_m)'_{GAR} = \frac{(k_{cat}/K_m)_{GAR}}{(1 + H/K_{S1})(1 + K_{ES2}/H)}$$

$$(k_{cat})' = \frac{k_{cat}}{(1 + H/K_{ES1S2} + K'_{ES1S2}/H)}$$

[a] Rate equations were derived using the assumption that the ionizations are at equilibrium and the addition and dissociation of substrates are at steady state conditions. The dissociation constants, K_{ES1} and K_{S1}, correspond to K_{a1} in eq 3, and K_{S2} and K_{ES2} correspond to K_{a2} in eq 3. The dissociation constants, K_{ES1S2} and K'_{ES1S2} correspond to K_{a1} and K_{a2} in eq 1, respectively.

and Asp144, are essential for catalysis. The K_m values of GAR and fDDF for both mutant enzymes are very similar to those of the wild type, suggesting that these mutations caused no significant changes either in the structure or in the binding of the substrates and intermediates. Like the wild type enzyme, both mutants exhibited no irreversible inactivation upon changing pH values. Therefore, the k_{cat}−pH profiles for these mutants must result from the changes in the active site environment caused by the mutations.

It appears that both His108 and Asp144 are responsible for the pK_a of 9.7. The pH dependence of k_{cat} requires that the side chain group responsible for the pK_a of 9.7 be protonated to be more active. As shown in Figure 3, His108 is the only ionizable group that forms a hydrogen bond directly to the formyl oxygen. We conclude that the pK_a of 9.7 represents His108 that acts as a general acid catalyst. The unusually high pK_a value for the imidazole of H108 must arise from hydrogen bonding to Asp144. This hydrogen-bonding interaction implies that these two residues would be interdependent in the catalytic mechanism. Although His108 is still present in the D144A mutant, the absence of the aspartic acid may cause a misalignment of the imidazole. A mutation of either residue should impair the catalytic role of His108, which would lead to the loss of the pK_a of 9.7 in the k_{cat}−pH profile for the wild type.

Another important requirement in the formation of the tetrahedral intermediate is the ionization of the amino group of GAR whose pK_a is known to be 8.15 (*14*). In a low-dielectric environment such as the active site of an enzyme, the pK_a value of the amino group may be lowered relative to that measured in water. Therefore, the most likely candidate for the group with a pK_a of 6.8 should be the amino group of GAR in the ternary complex. Several lines of evidence support this assignment. In the k_{cat}−pH profile, the moiety with a pK_a value of 6.8 must be unprotonated to be more active, as should the amino group of GAR to act as a nucleophile. All the mutants that were studied exhibit very similar pK_a values in the acid leg of the k_{cat}−pH profiles, indicating that this pK_a value represents the same moiety for both the wild type and mutant enzymes and is attributed to the amino group of GAR. Additional evidence is derived from k_{cat}/K_m profiles (vide infra) because the assignment of

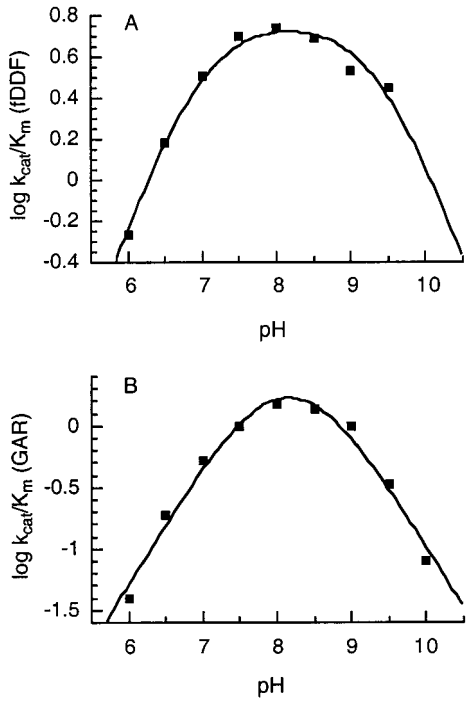

FIGURE 4: pH dependence of k_{cat}/K_m(fDDF) (A) and k_{cat}/K_m(GAR) (B) for the wild type enzyme. The curves are fitted to eq 3.

a pK_a value to substrate ionization in the ternary complex may accompany its appearance in the k_{cat}/K_m−pH profiles (Scheme 1) (*15*, *16*).

pH Dependence of k_{cat}/K_m(fDDF). The k_{cat}/K_m(fDDF)−pH profile also describes a bell-shaped curve with the limiting slope of 1 on either side of the curve (Figure 4A). The calculated pK_a values obtained from curve fitting to eq 3 were 7.0 ± 0.1 and 9.4 ± 0.1. Similar pK_a values were obtained in the pH profiles for the mutant enzymes (Table 2). These two pK_a values should represent the ionization of groups found in the free enzyme (in this case, the E−GAR complex) or the free substrate (fDDF). The acid side pK_a value for each mutant or the wild type enzyme overlaps with the corresponding pK_a value in its k_{cat}−pH profile. This pK_a must represent the ionization of the amino group of GAR in the E−GAR complex responsible for catalysis, consistent with an active site environment similar to that of the ternary

Table 2: Summary of pK_a Values for GAR Transformylase

	k_{cat}	k_{cat}/K_m(GAR)	k_{cat}/K_m(fDDF)
wild type	6.8 ± 0.1, 9.7 ± 0.1	7.8 ± 0.2, 8.6 ± 0.2	7.0 ± 0.1, 9.4 ± 0.1
H108A	6.9 ± 0.1	8.0 ± 0.2, 8.8 ± 0.3	6.7 ± 0.1, 9.4 ± 0.1
D144A	6.5 ± 0.1	7.6 ± 0.1, 8.8 ± 0.1	6.3 ± 0.1, 9.4 ± 0.1
H121Q	6.6 ± 0.1, 9.7 ± 0.2	7.9−8.0, 7.9−8.0	*a*

[a] Insufficient data to determine pK_a.

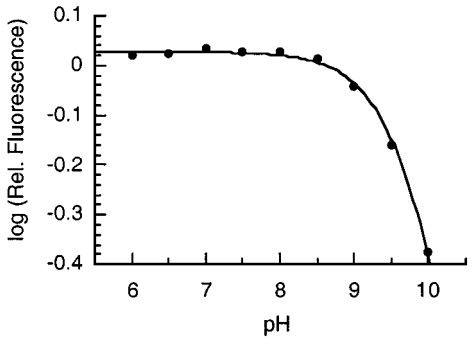

FIGURE 5: pH titration of fDDF monitored by fluorescence change at 400 nm with excitation at 340 nm. The curve is fitted to eq 4.

complex. This pK_a is expected to appear in the k_{cat}/K_m−pH profile when the substrate ionization has been assigned in the k_{cat}−pH profile for the ternary complex (Scheme 1).

The second pK_a of 9.4 is also very close to the corresponding pK_a value in the k_{cat}−pH profile for the wild type. Initially, we considered the possibility that this value might represent the ionization of His108-Asp144 responsible for catalysis as assigned in the k_{cat}−pH profile. However, a similar pK_a value was observed in the k_{cat}/K_m(fDDF)−pH profiles for H108A and D144A that lack one member of the catalytic pair. The absence of a second ionization, i.e., a slope of −2, in the descending leg of the k_{cat}/K_m(fDDF)−pH profile for wild type further indicates that this pK_a value may not at all be associated with the catalytic group, His108-Asp144, in the binary enzyme (the E−GAR complex). Indeed, examination of the X-ray structures of the apoenzyme and liganded enzyme revealed that the hydrogen-bonding interaction between these two side chain residues required the presence of a folate analogue. Since this pK_a value is only present in the k_{cat}/K_m(fDDF)−pH profile, it may represent a group for binding of cofactor.

This pK_a most likely is derived from fDDF since the interactions between the bound cofactor and enzyme consist primarily of hydrogen bonding with backbone amide residues that should not exhibit any pH dependence. Figure 5 displays the pH titration curve of fDDF in the pH range of 6.0−10.0, monitored by fluorescence change at 400 nm with excitation at 340 nm. The pH-dependent change in the fluorescence signal was fit with a pK_a value of 9.80 ± 0.02. This is attributed to the ionization of the amide moiety in the pterin ring of fDDF, since similar values have been assigned to this function in other folate compounds (*17*). Crystallographic data revealed that the 4-oxo and N3 of the pterin ring of folate make hydrogen bonds to the backbone nitrogen of Asp144 and the backbone oxygen of Thr140, respectively, indicating that the ionization of the amide moiety should affect the binding of folate (*5*). Asp144 seems to be brought into the active site after a flexible loop of residues 141−145 folds over the folate binding site upon binding of folate.

pH Dependence of k_{cat}/K_m(GAR). Figure 4B shows the pH profile of k_{cat}/K_m for GAR. Plotting of the logarithms of k_{cat}/K_m values against pH gave a slope of close to 1 on either acidic or basic limb, and curve fitting with eq 3 yielded two pK_a values, 7.8 ± 0.2 and 8.6 ± 0.2. Because the two pK_a values are very similar (within 1 pH unit), they were also estimated by the procedure of Alberty and Massey (*18*) and gave similar values. The H108A and D144A mutant enzymes exhibited very similar pH profiles and pK_a values (Table 2). These pK_a values may represent the ionization of groups in the free enzyme (in this case, the E−fDDF complex) or the free substrate (GAR). The group with a pK_a of 7.8 must be unprotonated, and the second group with a pK_a of 8.6 must be protonated either for catalysis or for the binding of GAR. The most likely candidate for the pK_a of 7.8 is the amino group of GAR that has to be unprotonated for activity as its appearance in the k_{cat}/K_m−pH profile may be accompanied by the pK_a value for the substrate ionization in the k_{cat}−pH profile for the ternary complex (Scheme 1).

The observed pK_a value, however, is about 0.4 pH unit lower than the reported literature value for free GAR, 8.15 (*14*). The difference could be due to the fact that the literature value was measured at an unspecified temperature and ionic strength, which may be different from ours. The reported pK_a values for the amino group of other glycinamides include a pK_a value of 7.63 which is assigned to the amino group of 1,2-bisglycylamidoethane, 8.13 to that of a Gly-Gly dipeptide, and 7.91 to that of a Gly-Gly-Gly tripeptide (*19*). Thus, the pK_a value of the amino group of glycinamides lies in the range of 7.6−8.2. Another possibility is that the observed pK_a reflects the fact that the binding of GAR to E−fDDF is not at equilibrium. An estimate of the displacement from the true pK_a can be calculated from the ratio of the net rate constant for the reaction of the ternary complex to yield product to the net rate constant for dissociation of substrate [expressed as $\log(1 + k_{forward}/k_{reverse})$] (*20*) and may drop the pK_a by 0.23 unit (*13*).

The second group with a pK_a of 8.6, which is exhibited in both the wild type and mutant enzymes, should be within the E−fDDF complex, since GAR does not have any other groups with this pK_a value. Because the His108-Asp144 pair does not exist in the mutant enzymes, H108A and D144A, this pK_a cannot be assigned to this pair. The k_{cat}/K_m(GAR)−pH profile for the wild type has a limiting slope of −1 on its basic limb, indicating that the profile may not exhibit a pK_a value for the catalytic group, His108-Asp144, in the E−fDDF complex. We surmise that the absence of GAR may obviate the function of the His108-Asp144 pair or shift its pK_a outside of the observable range. This pK_a may reflect a group responsible for binding common to all enzyme species.

A likely candidate for this group was sought by examination of the recently determined X-ray structures of apo-GAR transformylase (E70A) at pH 3.5 and 7.5 (*12*). A loop spanning residues 111−131 was found to undergo a pH-dependent conformational change upon comparison of the two structures. This loop is disordered and unresolved at pH 3.5 but transforms to an ordered loop−helix structure at pH 7.5. The structure of the ternary complex also has a well-defined loop conformation of residues 111−131 (*5*). These crystallographic studies suggest that the loop ordering is pH-dependent and may be important in catalysis and the binding

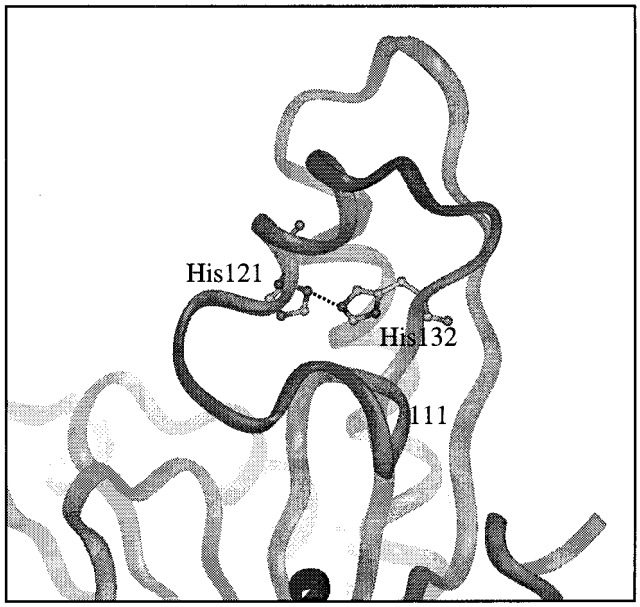

FIGURE 6: Fully ordered structure of the loop spanning residues 111−131 and the hydrogen bonding between His121 and His132 in the crystal structure of the apo-GAR transformylase (E70A) at pH 7.5 (*12*).

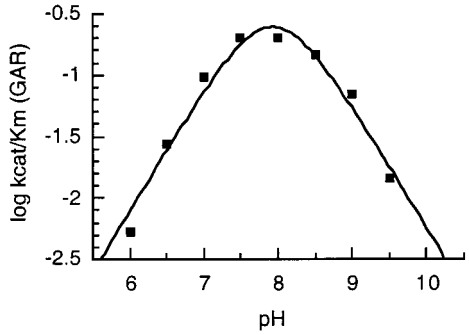

FIGURE 7: pH dependence of k_{cat}/K_m(GAR) for the H121Q mutant. The curve is fitted to eq 2.

of substrates. The loop is structured through hydrogen bonds, mostly involving main chain carbonyls and amide nitrogens and a few involving amino acid side chains. Of these side chains, His121 or His132 which hydrogen bond to each other appear to be the only residues that may have pK_a values within our pH range (Figure 6). Although we aware that any pK_a associated with a conformational change may result from a combination of the ionization of several groups, we decided to prepare the H121Q mutant enzyme, which is expected to retain a loop-stabilizing hydrogen bond, although differing in its stability toward pH changes.

The activity of H121Q is comparable to that of the wild type enzyme as its k_{cat} values are within 60% of those of the wild type (Table 1). The pH profile of k_{cat} is very similar to that of the wild type, as are the pK_a values (Table 2). However, K_m values for GAR and fDDF exhibit about 4-fold increase (Table 1). The pH profile of k_{cat}/K_m(GAR) for H121Q is bell-shaped but much narrower than that of the wild type, giving two similar pK_a values in the range of 7.9−8.0 (Figure 7). It appears that the pK_a value on the basic side is shifted to 7.9−8.0 from 8.6−8.8 in the pH profiles for the wild type, H108A, or D144A, but the acid side pK_a is essentially unchanged. This implicates the pK_a of 8.6 as being important in stabilizing the loop conformation and its involvement in the binding of GAR. The unchanged acid side pK_a must represent the amino group of GAR. The high K_m for GAR precluded accurate measurements needed for establishing a k_{cat}/K_m(fDDF)−pH profile.

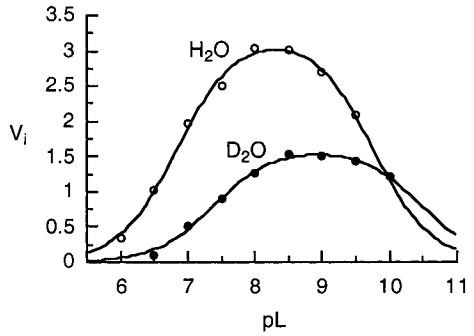

FIGURE 8: pL−rate profiles (L being H or D) for initial velocities (V_i) determined at saturating levels of GAR and fDDF in H_2O (○) and D_2O (●) buffers. The profiles are plotted as V_i vs pH to clearly show the shift of the pK_a values and the solvent isotope effect of 2, measured by $(V_i)_{max,H_2O}/(V_i)_{max,D_2O}$.

Solvent Deuterium Isotope Effect. Figure 8 shows the pL−rate profile (L being H or D) for initial velocities measured at saturating levels for both GAR and fDDF as a function of hydrogen and deuterium concentration. As expected, the pH−rate profile and the resulting pK_a values are exactly the same as those from the pH dependence of k_{cat}. In the pD profile, however, both pK_a values were shifted to higher values by about 0.6−0.8 pH unit, giving pK_a values of 7.4 ± 0.1 and 10.5 ± 0.1. The overall amplitude is approximately half that for the pH profile. The observed pK_a shift, 0.6, is consistent with the assignments of pK_a groups to the amino group of GAR and the imidazolium group of His108 since ammonium groups are expected to have a pK_a shift of 0.6 pH unit (*21*). The pL-independent D_2O solvent isotope effect was 2.0 ± 0.1, which indicates that a proton transfer is involved in the interconversion of the substrate and product ternary complexes.

DISCUSSION

Role of Active Site Residues. The active site residues, His108, Asp144, and Asn106, are strictly conserved among the prokaryote and eukaryote GAR transformylases. Although the structure of the active site has been well characterized and the importance of these residues has been demonstrated by site-directed mutagenesis, the exact role of the active site residues in transformylation has been largely speculative. Our current study clearly shows that His108 acts as a general acid catalyst in the formation of the tetrahedral intermediate with the pK_a value of 9.7. This unusually high pK_a value for His108 is due to the salt bridge with the carboxylate of Asp144 and consequently provides the enzyme with maximum catalytic efficiency at physiological pH. Therefore, Asp144 is absolutely required for the catalytic mechanism as it maintains the correct protonation state of the general acid catalyst, His108.

Asp144 may also position His108 in a correct conformation which seems to be induced by cofactor binding to interact with the formyl group of the cofactor. In the crystal structures of the apoenzyme, a flexible loop of residues 141−145 is positioned away from the active site (*5*, *6*, *12*). This

loop becomes stabilized in the folate-bound complexes and folds over the folate binding site as a result of the interaction of the amide moiety of the pterin ring with the backbone atoms of the loop (*5*, *6*). One consequence of this loop movement is the positioning of Asp144 in the active site in forming a hydrogen bond to His108, positioning the imidazole to hydrogen bond with the formyl oxygen of folate. This interplay of active site residues with the formyl group upon binding of the cofactor must be a critical determinant of the catalytic function of the enzyme.

The D144A mutant would forfeit the interaction with the imidazole of His108, and in turn disrupt the hydrogen bond between His108 and the formyl group of the cofactor. Binding of cofactor to this mutant may not be disturbed as the cofactor interacts only with the backbone atoms of the loop. In this mutant, the imidazole of His108 might favor an alternative conformation such as the one found in the crystal structure of the BW1476U89 multisubstrate adduct−GAR transformylase complex which involves hydrogen bonding between the imidazole nitrogens and the backbone carbonyl of Asp144 and the side chain of Ser135 (*6*). Such changes in the active site geometry of D144A could result in a comparable reduction of catalytic activity relative to that of the H108A mutant. The D144A mutant, however, has an even lower k_{cat} value by 1 order of magnitude than H108A. We note that the carboxylate of Asp144 hydrogen bonds with a water molecule in the crystal structure of the BW1476U89 multisubstrate adduct−GAR transformylase complex (*6*). It has been proposed that the water molecule functions as a catalyst for a proton transfer from the amino group of GAR to the N10 of folate (*6*). The loss of this pathway in the D144A mutant could result in its lower k_{cat} value.

The single-turnover experiments and the deuterium solvent isotope effect measurements established that the interconversion of substrate and product ternary complexes is rate-limiting in the kinetic sequence and is the step evaluated by k_{cat} over the pH range that is studied. The assignment of the pK_a of 9.7 in the k_{cat}−pH profile to His108 does not require a complete proton transfer from the protonated imidazolium to the oxyanion of the tetrahedral intermediate that could lead to the accumulation of an unproductive species (*7*). The pK_a of 6.8 in the k_{cat}−pH profile reflects the ionization of the amino group of GAR, another determinant in the formation of the tetrahedral intermediate. The appearance of the pK_a value of the amino group of GAR in the k_{cat}/K_m−pH profiles confirms this interpretation. Consequently, the enzyme should bind both the protonated and free base form of GAR (Scheme 1). The crystal structure of the ternary complex implicates the phosphoryl and the ribosyl hydroxyl groups in the binding of GAR (*5*). Thus, the ionization state of the amino group in GAR may not be a binding determinant.

Loop Conformations of Residues 111−131 and 141−145. Recent crystallographic studies have shown that a loop spanning residues 111−131 in the apoenzyme undergoes a pH-dependent conformational change from a completely disordered state at pH 3.5 to a fully ordered loop−helix structure at pH 7.5 (*12*). Because the ternary complex of enzyme with GAR and a folate analogue also exhibits a fully ordered loop of residues 111−131 (*5*), it has been proposed that the ordering of this loop might be responsible for the

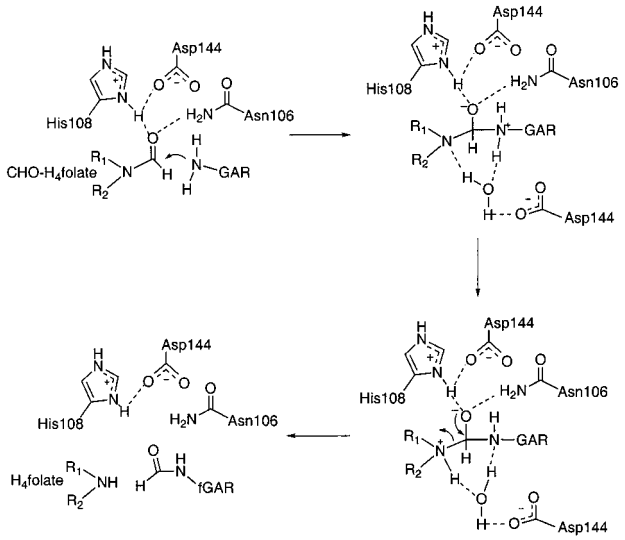

FIGURE 9: Proposed mechanism for GAR transformylase. As the cofactor binds to the active site, Asp144 forms a salt bridge to the imidazolium of H108 and the formyl group is positioned to form hydrogen bonds to Asn106 and the protonated imidazolium group of H108. The free base form of the amino group of GAR then attacks the activated formyl group to form a tetrahedral intermediate. A proton transfer from GAR to the N10 of folate is mediated by a catalytic water molecule, followed by breakdown of the tetrahedral intermediate to form products. The positioning of this water molecule may be assisted by a hydrogen bond to the carboxylate of Asp144. (For clarity, we show Asp144 twice; it actually spans from the N1 of His108 to the bound H_2O molecule.)

observed pH-dependent behavior of enzyme activity. However, under saturating conditions the low activity at the lower pH values is due to the unfavorable ionization of the nucleophile of the substrate and at higher pH values to the dissociation of the H108-D144 salt bridge. This suggests that the loop conformation of residues 111−131 is not a determinant of enzyme activity under saturating conditions. In fact, the loop mutant H121Q, although it exhibited higher K_m values for both GAR and fDDF than the wild type, yielded k_{cat} and pK_a values in the k_{cat}−pH profile similar to those of the wild type.

The loop conformation of residues 111−131, however, may act in the binding of substrates and impact k_{cat}/K_m. We infer that the pK_a for structured loop formation should lie around pH 7, since all the crystal structures determined below pH 6.75 have a disordered loop whereas those determined above pH 7.5 have an ordered loop. The k_{cat}/K_m(GAR) profile did not reflect a pK_a value around pH 7, but implicated pK_a values of 7.6 and 8.8 that were assigned to the amino group of free GAR and the loop, respectively. The shift of the latter pK_a to 8.3 in the H121Q mutant supports this assignment. This indicates that the loop conformation in the E−fDDF complex at high pH may not favor GAR binding and may differ in its behavior from that observed with the apoenzyme. We conclude that the loop conformation of residues 111−131 affects the binding of the substrate and thus the pH dependence of the enzymic activity.

Likewise, the loop conformation of residues 141−145 is a determinant of catalytic activity. Its positioning requires the presence of folate, which is manifested in the k_{cat}/K_m-(fDDF) profile that reflects, in the wild type and mutant enzymes, the ionization of the N3 proton of the folate cofactor. Loss of this proton apparently leads to disrupting

an interaction with the amide backbone of this loop and loss of activity owing to misalignment of the active site residues, His108 and Asp144.

Chemical Mechanism. Our proposed mechanism is depicted in Figure 9. Folate binding induces active site rearrangements involving Asp144 and H108, which place the protonated imidazolium partnered in a salt bridge to the carboxylate in a position to activate the formyl group of the cofactor by donating a proton to the formyl oxygen. Asn106 also interacts with the folate, and may fine-tune the location of the formyl group. A low-dielectric active site environment favors the free base form of the amino group of GAR, poised to attack the activated formyl group to form presumably a tetrahedral intermediate in the transfer process. A proton is switched from GAR to the N10 of folate mediated by a catalytic H_2O molecule, followed by breakdown of the tetrahedral intermediate and product release. The positioning of the catalytic H_2O molecule may also be assisted by Asp144.

The key feature in this mechanism is the general acid catalysis by His108. It has been well established that acid−base catalysis is important in an acyl transfer mechanism. We speculate that the formyl group is activated for transfer not only by proton donation from His108 but also perhaps by twisting the formyl group out of the delocalized planar structure to relieve the resonance stabilization. Studies are underway to find physical evidence for such preactivation of the formyl group in the enzyme's active site.

REFERENCES

1. Smith, J. M., and Daum, H. A., III (1987) *J. Biol. Chem. 262*, 10565−10569.
2. Inglese, J., Johnson, D. L., Shiau, A., Smith, J. M., and Benkovic, S. J. (1990) *Biochemistry 29*, 1436−1443.
3. Daubner, S. C., Young, M., Sammons, R. D., Courtney, L. F., and Benkovic, S. J. (1986) *Biochemistry 25*, 2951−2957.
4. Kan, C. C., Gehring, M. R., Nodes, B. R., Janson, C. A., Almassy, R. J., and Hostomska, Z. (1992) *J. Protein Chem. 11*, 467−473.
5. Almassy, R. J., Janson, C. A., Kan, C.-C., and Hostomska, Z. (1992) *Proc. Natl. Acad. Sci. U.S.A. 89*, 6114−6118.
6. Klein, C., Chen, P., Arevalo, J. H., Stura, E. A., Marolewski, A., Warren, M. S., Benkovic, S. J., and Wilson, I. A. (1995) *J. Mol. Biol. 249*, 153−175.
7. Warren, M. S., Marolewski, A., and Benkovic, S. J. (1996) *Biochemistry 35*, 8855−8862.
8. Mueller, W. T., and Benkovic, S. J. (1981) *Biochemistry 20*, 337−344.
9. Smith, G. K., Mueller, W. T., Slieker, L. J., and Benkovic, S. J. (1982) *Biochemistry 21*, 2870−2874.
10. Inglese, J., Smith, J. M., and Benkovic, S. J. (1990) *Biochemistry 29*, 6678−6687.
11. Mullen, C. A., and Jennings, P. A. (1996) *J. Mol. Biol. 262*, 746−755.
12. Su, Y., Yamashita, M. M., Greasley, S. E., Mullen, C. A., Shim, J. H., Jennings, P. A., Benkovic, S. J., and Wilson, I. A. (1998) *J. Mol. Biol. 281*, 485−499.
13. Shim, J. H., and Benkovic, S. J. (1998) *Biochemistry 37*, 8776−8782.
14. Hartman, S. C., Levenberg, B., and Buchanan, J. M. (1956) *J. Biol. Chem. 221*, 1057−1070.
15. Tipton, K. F., and Dixon, H. B. F. (1979) *Methods Enzymol. 63*, 183−234.
16. Laidler, K. J. (1955) *Trans. Faraday Soc. 51*, 528−539.
17. Poe, M. (1977) *J. Biol. Chem. 252*, 3724−3728.
18. Alberty, R. A., and Massey, V. (1954) *Biochim. Biophys. Acta 13*, 347−353.
19. Perrin, D. D. (1965) *Dissociation Constants of Organic Bases in Aqueous Solution*, Butterworths, London.
20. Cleland, W. W. (1977) *Adv. Enzymol. 45*, 273−387.
21. Schowen, K. B., and Schowen, R. L. (1982) *Methods Enzymol. 87*, 551−606.

BI9904609